DE85 010442

ORNL/TM-9542 Distribution Category UC-20d

Engineering Physics and Mathematics Division

MAGNETICS CALCULATIONS FOR AN ELMO BUMPY SQUARE*

R. T. Santoro, N. A. Uckan, and R. J. Schmitt

*Submitted for Journal publication

⁺Fusion Energy Division

[†]McDonnell Douglas Astronautics Co.

Date of Issue: March 1985

Research sponsored by U.S. Dept. of Energy Office of Fusion Energy

Prepared by the
Oak Ridge National Laboratory
Oak Ridge, Tennessee 37831
operated by
Martin Marietta Energy Systems, Inc.
for the
U.S. DEPARTMENT OF ENERGY
under Contract No. DE-AC05-840R21400

overnment. Neither the United States Government nor any agency thereof, nor any of their nployees, makes any warranty, express or implied, or assumes any legal liability or responsitive for the accuracy, completeness, or usefulness of any information, apparatus, product, or occas disclosed, or represents that its use would not infringe privately owned rights. Reference berein to any specific commercial product, process, or service by trade name, trademark, anufacturer, or otherwise does not necessarily constitute or imply its endorsement, recompatition, or favoring by the United States Government or any agency thereof. The views d opinions of authors expressed herein do not necessarily state or reflect those of the nited States Government or any agency thereof.



DISCLAIME

TABLE OF CONTENTS

ABSTRACT	V
I. INTRODUCTION	1
II. EBS CONFIGURATION	1
III. DISCUSSION	2
A. Method of Calculation	
B. Magnetics	
C. Magnetic Forces	
D. Trim Coil Control	
IV. CONCLUSIONS	10
Deferences	13

MAGNETICS CALCULATIONS FOR AN ELMO BUMPY SQUARE

R. T. Santoro and N. A. Uckan
Oak Ridge National Laboratory, Oak Ridge, TN 37831

R. J. Schmitt
McDonnell Douglas Astronautics Company, St. Louis, MO 63166

ABSTRACT

Calculations have been carried out to determine the vacuum magnetic parameters, forces, and the use of trim coils in an ELMO Bumpy Square. A configuration having five mirror coils per side and an eight-coil high-field toroidal solenoid corner assembly was studied. Favorable magnetic parameters are achieved in the device. An on-axis mirror ratio of 1.9, a global mirror ratio of 3.6, and excellent centering of plasma pressure contours are achieved. Particle losses are also minimal (<5%). The magnetic forces acting between coils are comparable with those encountered in the EBT-I/S magnet configuration. Circular trim coils were found to be suitable for restoring hot electron ring locations that are displaced when the coil current are varied for performing magnetic studies or for assessing the effects on the EBS of the global mirror ratio.

I. INTRODUCTION

Advanced ELMO Bumpy Torus (EBT) concepts have been studied in an effort to determine the potential for new and different concepts as confinement experiments or as reactors. Several magnetic configurations based on the EBT confinement concept were developed including the ELMO Bumpy Square (EBS) first introduced by L. W. Owen in 1982. The EBS was selected for near-term study on the basis of its (1) ability to address and resolve critical EBT issues in a cost-effective manner, (2) intrinsic desirability as a reactor configuration, and (3) potential contribution to the physics and technology of fusion, in general.²

A comprehensive theoretical and engineering analysis of the EBS concept was carried out to assess the merits of the EBS configuration with respect to particle confinement, heating, transport, ring production, and stability.³ The study focused on a design involving modification and reconfiguration of the EBT-I/S. That is, a reconfiguration of the toroidal EBT-I/S magnet-vacuum vessel geometry into a square geometry having dimensions that allow its incorporation into the EBT-I/S enclosure. This paper summarizes the results of calculations that were carried out to provide data for assessing the vacuum magnetic parameters of the EBS and to provide information to aid in the mechanical design of the magnet support structure and containment for the coils.

II. EBS CONFIGURATION

The EBS configuration consists of four linear arrays of simple mirrors that are connected by 90° sectors of a high-field toroidal solenoid. Figure 1 shows the geometry of one quadrant of the EBS. The device is comprised of twenty of the existing EBT-I/S mirror coils, five to each side, with a mirror ratio of 1.9. The mirror sector length (the coil spacing) in the sides is $L_{\rm M}=40$ cm. The connecting corner sections are constructed using eight newly designed half-size EBT mirror coils that generate a magnetic field with negligible ripple in the corners. The major radius of the corner sections is $R_{\rm corner}=44$ cm with the axis at each corner displaced radially outward by $(\Delta_{\rm shift})_{\rm corner}=2.5$ cm from the axis of the sides. The outward displacement of the corner coils and the distance between the mirror coils and the turning coils, called the transition sector, $L_{\rm TR}$, are adjusted so that hot electron rings are formed in the transition sector on the same flux lines as in the axisymmetric sectors. In the geometry shown in Fig. 1, $L_{\rm TR}=42$ cm. All of the coils have an inside radius of 16.36 cm. The side mirror coils have a cross-sectional area of 10.16 x 7.30 cm² and carry a current of 7777 A in 44 turns. The corner coils carry 9000 A in 22 turns and the cross-sectional area is 5.08 x 7.30 cm².

Most of the calculations were performed using the geometry shown in Fig. 1. Also considered was a geometry including circular "trim-coils" positioned coaxially in the center of the transition sector. The inside radius of these coils was 32.7 cm with cross-sectional area of 2.65 x 2.65 cm². The trim coils are used to restore the ring location in the transition region when the currents flowing in the mirror and corner coils are varied to study magnetic performance or to assess the effects of the global mirror ratio.

ORNL-DWG 84-2753A2 FED

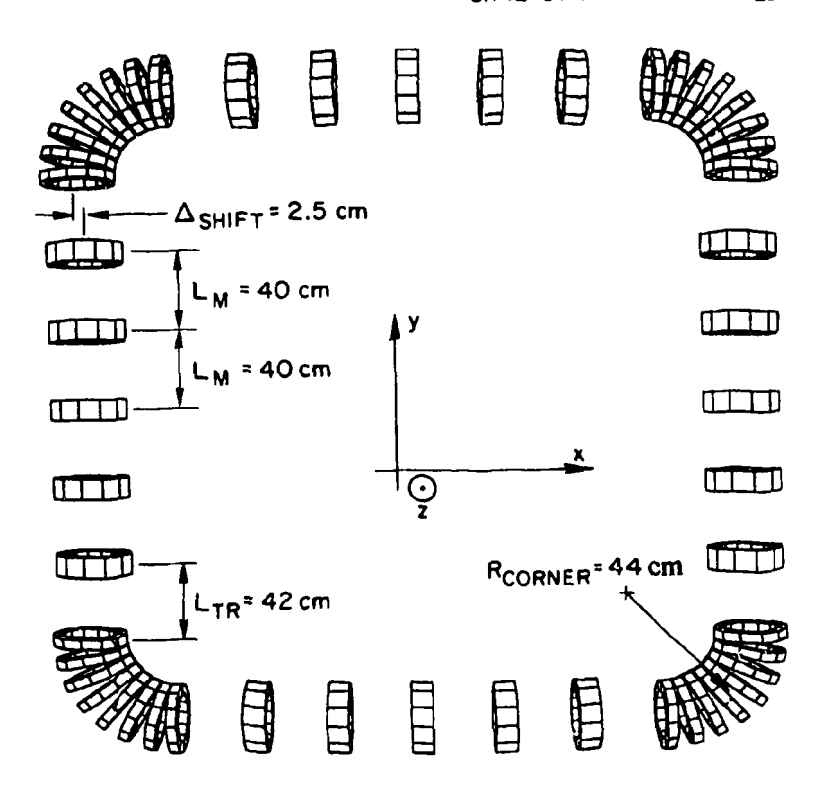


Fig. 1. Geometry of the EBS configuration indicating the coil arrangement.

III. DISCUSSION

A. Method of Calculation

The magnetic parameters for the EBS configuration were determined with the computer code EFFI,⁴ which calculates the magnetic flux lines, fields, forces, and inductance for an arbitrary system of coils defined using circular arcs and/or straight segments of conductors of rectangular cross section. The methods used for the calculation are based on a combination of numerical and analytical integration of the Biot-Savart Law for a volume distribution of current. The solutions yield accurate field values inside and outside the conductors. The magnetic field at a point in space, p, produced by a volume distribution of current is obtained from the relation

$$\overline{B}(p) = \frac{J\mu_0}{4\pi} \int_{s} \int_{s} \frac{d\overline{l} \times (\overline{r}_2 - \overline{r}_1)d\overline{s}}{|\overline{r}_2 - \overline{r}_1|}$$
(1)

where J is the current density in the conductor and μ_0 is the permeability of free space. In Eq. (1), \bar{r}_1 is the source position vector, \bar{r}_2 is the field position vector, $d\bar{l}$ is the vector differential element in the direction of the current flow, and $d\bar{s}$ is a differential area element perpendicular to the current flow.

The magnetic flux lines are defined by solutions to the differential equation

$$dy_i / | d\bar{s} | = B_{y_i} / | \bar{B} | \qquad (2)$$

and the magnetic force exerted on a coil is calculated by integrating the vector product \overline{J} x \overline{B} over the conductor volume

$$\overline{F} = \int_{1}^{\infty} \int_{S} Jd\overline{l} \times \overline{B} ds$$
 (3)

B. Magnetics

The magnetic field lines (solid curves) and the mod-B contours (dotted curves) in the equatorial plane of the EBS are given in Fig. 2. The 2.5 cm outward displacement of the corner coils with respect to the mirror coil axis symmetrizes the mod-B in the transition sector relative to the axis of the mirror section. Thus, the electron rings are formed consistently on the same flux lines throughout the device. It can also be observed that incorporating eight half-size coils in the corner results in negligible (< 0.5%) ripple in the field lines in the corner and that there is no observable perturbation even in the outermost flux lines that just graze the coil winding. The magnetic field strength as a function of distance along the magnetic axis is shown in Fig. 3. These data show the on-axis mirror ratio (B_{max}/B_{min}) to be \approx 1.9 and the global mirror ratio (B_{corner}/B_{side}) to be \approx 3.6.

The core plasma pressure contours (constant fdl/B) and passing particle drift orbits (contours of constant fdl) are shown in Figs. 4 and 5, respectively. For small mirror radii, the pressure contours are centered at $x \approx -1.2$ cm. The pressure contours become progressively more centered about the mirror axis for larger values of the minor radius. The orbits of deeply trapped particles $(v_{\parallel}/v=0)$ and the fdl/B contours will tend to coincide and be nearly centered on the mirror axis in an EBS.² This centering further implies that the hot electron rings will also be well centered forming in nearly axisymmetric fields.

Shown in Fig. 6 is the filling factor as a function of v_{\parallel}/v . The filling factor, or volumetric efficiency, is the ratio of the area of the drift orbit that passes through the limiting flux line in the midplane for a given pitch angle to the area intercepted by the limiter. The limiter is taken to be a circle in the midplane defined by projecting the coil throat along the lines. The data in Fig. 6 were obtained for a limiter having a radius of 11 cm. The filling factor is a figure of merit since it can be interpreted as a measure of particle losses caused by unconfined drift orbits which intercept the walls of the vacuum chamber.

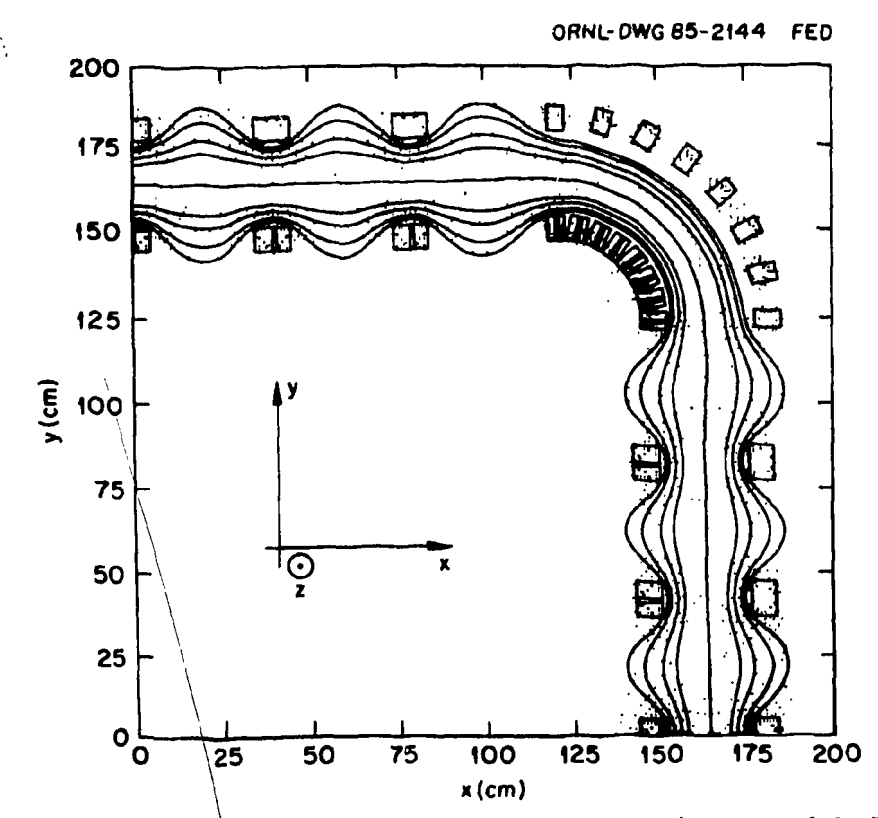


Fig. 2. Magnetic field lines and mod-B contours in the equatorial plane of the EBS.

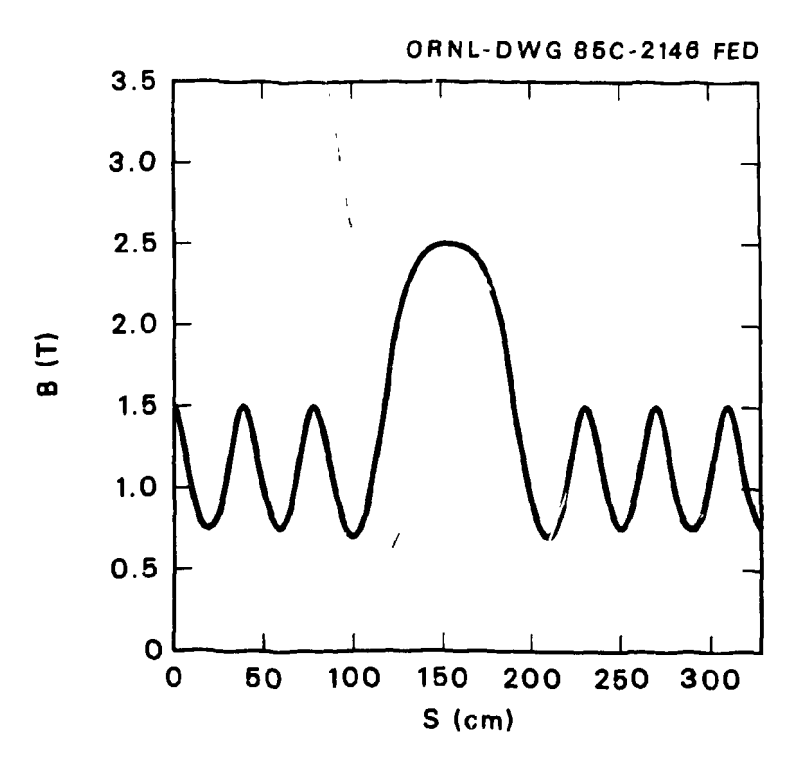


Fig. 3. Magnetic field strength versus arc length along the magnetic axis.

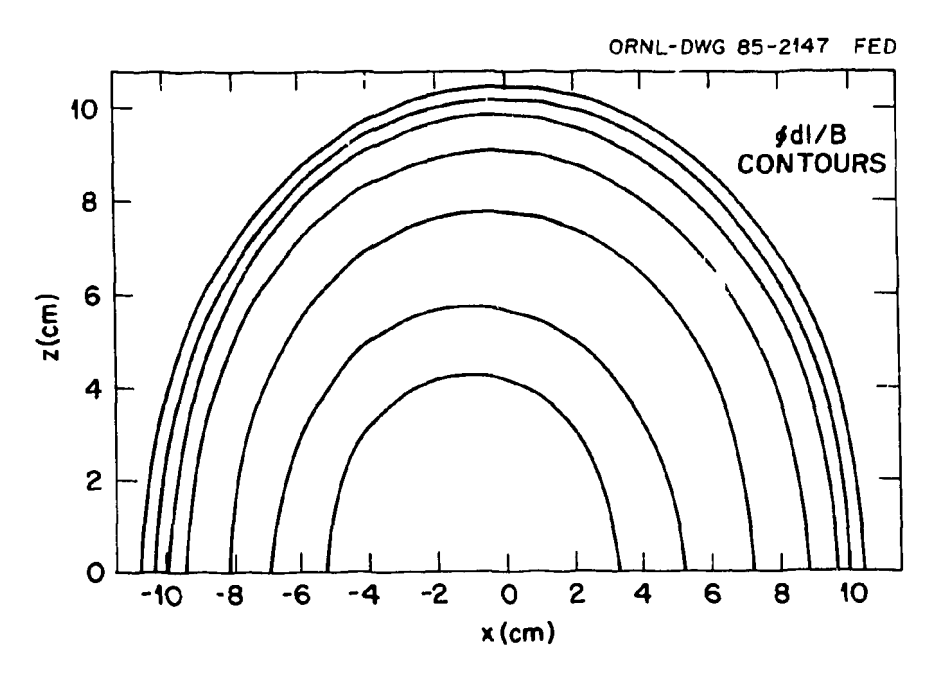


Fig. 4. Core plasma pressure contours in the coil midplane of the EBS (contours of constant fdl/B).

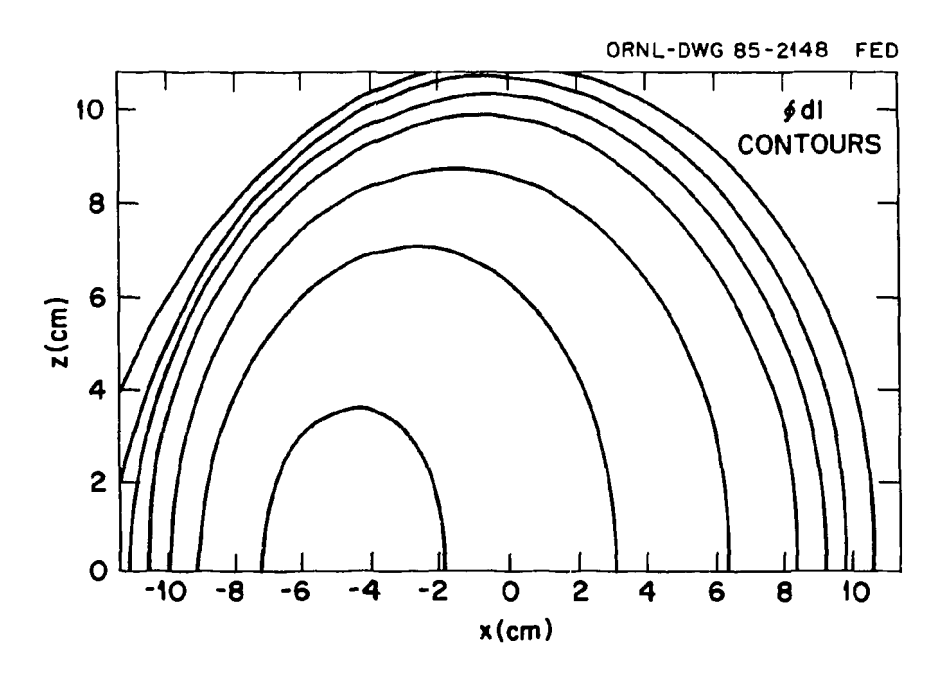


Fig. 5. Passing particle drift orbits in the coil midplane of the EBS (contours of constant fdl).

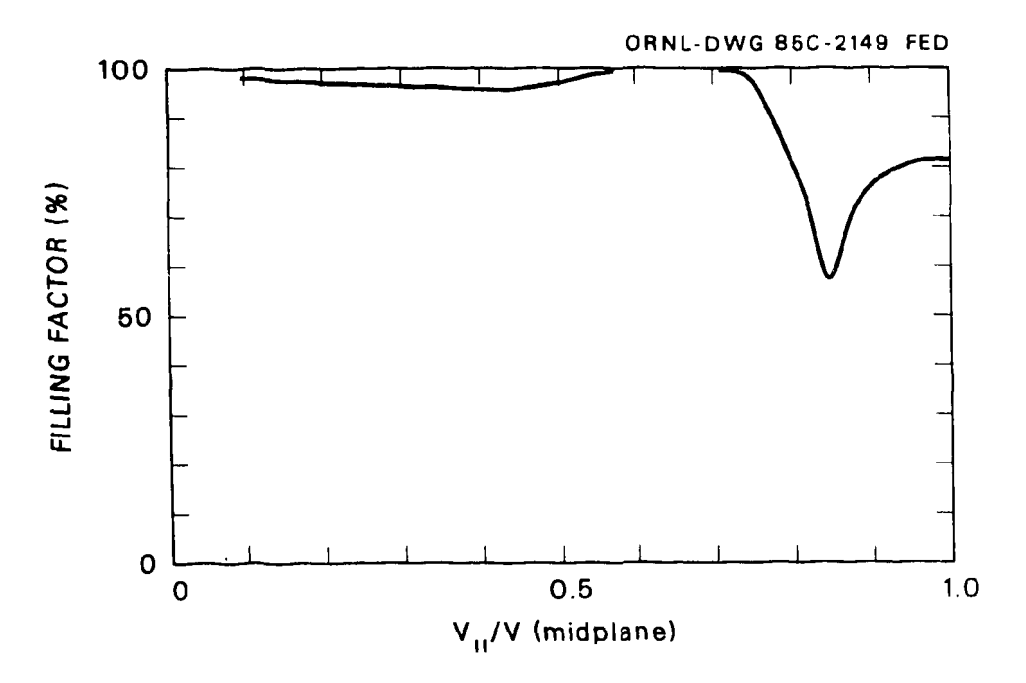


Fig. 6. Filling factor versus V_{\parallel}/V at the midplane of the EBS.

In Fig. 6, v_{\parallel}/v is defined in the midplane. The point to note from these data is that the area for the trapped particles, $v_{\parallel}/v = 0$, is nearly unity and that as particles become more passing, $v_{\parallel}/v \rightarrow 1$, the volumetric efficiency still remains large, and the particle losses in an EBS are small (<5%). In the EBT toroidal configuration, the maximum value of the filling factor is ~ 0.5 at $v_{\parallel}/v = 0$ and particle losses of $\sim 50\%$ are normal.

C. Magnetic Forces

The mechanical design of the EBS must take into account the forces acting on the coils due to the magnetic field and the steady current distribution in the coils. The coil support structure must be designed to maintain the weight of the coils and also to sustain the mechanical rigidity and alignment of the magnets in the presence of these forces so that no deflection or displacement of the coils occurs during operation.

The case of each mirror coil is directly supported by a stand that is bolted to the floor. The corner coils are similarly supported. The individual stands are appropriately coupled to distribute and maintain centering and out-of-line magnetic forces over the centerline span of the device.

The components of the total magnetic forces acting on the transition and corner coils are summarized in Fig. 7. The z-component of the forces have been omitted since they are very small (~10⁻⁹ lbs). The calculated forces are comparable with those found on the EBT-I/S device so no extraordinary supports are required for the EBS. The components of the magnetic forces vary from a few pounds to several tons with the largest forces acting on the corner coils just adjacent to the transition section.

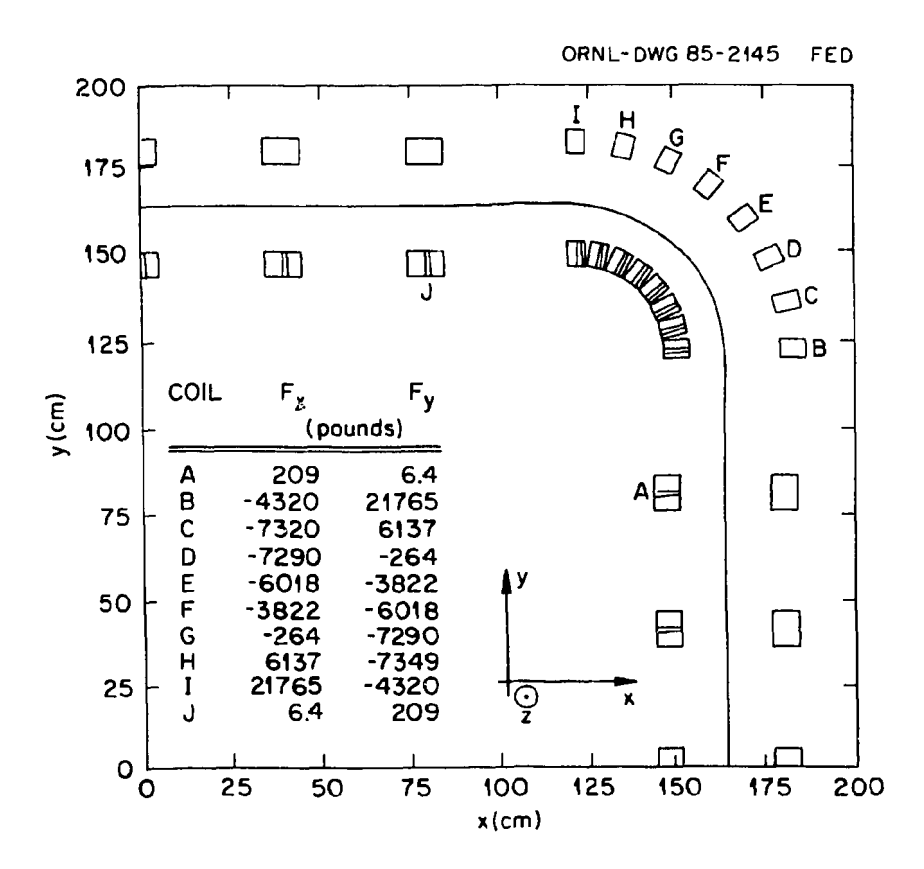


Fig. 7. Magnetic force distribution in the transition and corner coils of the EBS.

The data given in Fig. 7 are the total x and y components of the magnetic force. In determining these data, the coil is divided into twelve elements and the components of the forces are separately calculated for each element. These data permit the EBS designers to estimate the torque acting on each magnet. Table 1 summarizes the components of the force on each element for coils A and B in Fig. 7.

D. Trim Coil Control

All of the previously discussed calculations were carried out for the EBS configuration shown in Fig. 1. For currents flowing in the mirror and corner coils of 7777 A and 9000 A, respectively, and for the transition sector length of 42 cm, the hot electron rings are formed on the same flux line in the mirror and transition sections. The rings are formed at the intersection of the second harmonic mod-B surface and magnetic field line having a minimum of 0.5 T. The currents supplied to the mirror and corner coils may be varied to study magnetic parameters or the effects of global mirror ratio. Altering the current perturb the field line mod-B configuration and the ring location in the transition sector relative to the mirrors. Restoring the ring location is accomplished with the use of trim coils.

Table 1. Elemental Forces Acting on Coils A and B

Current element	E	E	.
	F _x	F _y	F _z
		(pounds)	
	•	Coil-A	
1	-3893.0	38.3	-1043.3
	-2856.7	26.3	-2857.3
2 3	-1049.4	7.6	-3198.6
4	1055.0	-11.0	-3935.2
4 5	7891.3	-25.2	-2890.7
6	3957.0	-32.7	-1060.1
6 7	3957.0	-32.7	1060.1
8	2891.3	25.2	2890.7
9	1055.0	-i1.0	3935.2
10	-1049.4	7.6	3198.6
11	-2856.7	26.3	2857.3
12	-3893.0	38.3	1043.3
		Coil-B	
1	-3644,9	2487.4	-969.9
	-2444.6	2210.8	-2424.9
2 3 4	-794.8	1862.1	-2916.1
4	686.3	1584.8	-2596.2
5	1745.4	1409.8	-1752.9
6	2292.8	1327.3	-615.9
7	2292.8	1327.3	615.9
8	1745.4	1409.8	1752.9
9	686.3	1584.8	2596.2
10	-794.8	1862.1	2916.1
11	-2444.6	2210.8	2424.9
12	-3644.9	2487.4	969.9

The effects of trim coils on the maintenance of the ring location is studied here. As noted above, circular trim coils having a radius of 32.7 cm and centered in the transition sector were considered. The trim coils have a cross-section area corresponding to $\sim 10\%$ of that of the mirror coils. The location of the coils optimizes their function and has the smallest effect on space conflicts with other systems and components.

The relationship between coil current and the trim coil current required to keep the rings on the same flux line in the transition sector as in the mirror sector is shown in Fig. 8. The reference ring location is indicated on the solid curve and is produced by the current conditions given above. Changes in the corner coil current move the ring location along the solid line. That is, the second harmonic mod-B surface in the transition sector moves relative to its location in the mirror section by the amount indicated on the ordinate. In the reference case, the ring forms in the transition sector at a distance r_{ref} from the mirror axis. Decreasing the corner coil current moves the ring closer to the axis in the transition sector while its location in the mirror sector remains at r_{ref} . For a decrease in corner coil current, the ring location is restored by supplying the trim coil with a fraction of the current flowing in the mirror coil. If the corner coil current is reduced to 8300 A, the ring location may be restored by supplying the trim coil with 25% of the current fed to the mirror coil. The plus sign means that the current in the trim coil flows in the same direction as in the mirror coil. If the corner coil exceeds 9000 A, the current to the trim coils must flow opposite to that in the mirror coil to restore the ring location at the reference location.

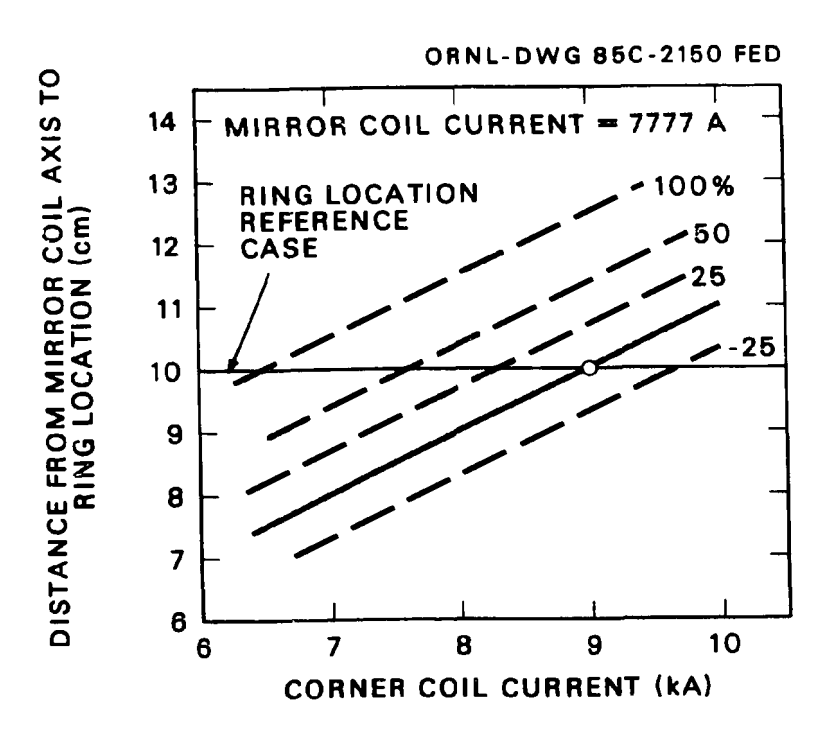


Fig. 8. Trim coil currents required to restore hot electron ring location due to changes in the corner coil currents.

IV. CONCLUSIONS

The ELMO Bumpy Square represents a viable alternative to the EBT. Calculations indicate that favorable magnetic parameters can be achieved. An eight-coil corner assembly couples the linear mirror sectors with negligible field line ripple (< 0.5%). The axisymmetric sector mirror ratio is ~1.9 while the global mirror ratio, (B_{corner}/B_{side}), is ~3.6. Particle drift orbits are considerably better centered for trapped, passing, and transitional particles in the EBS than in the EBT. In addition, nearly 95% of the particles are confined compared to ~50% for the EBT. The hot electron rings are formed in nearly axisymmetric fields consistently in the mirror and transition sectors and the ring locations are readily maintained with the use of circular trim coils placed coaxially with the mirror axis and centered in the transition sector.

The magnetic forces acting between coils are comparable with those encountered in the EBT and reconfiguration of the toroidal coil assembly can be accomplished using existing magnet support structures.

References

- 1. L. W. OWEN, D. K. LEE, and G. L. HEDRICK, "ELMO Bumpy Square," in Advanced Bumpy Torus Concepts Proceedings of the Workshop, CONF-830758, Oak Ridge National Laboratory (1983).
- 2. N. A. UCKAN, "EBT Advanced Concepts-Status Report," January 1984 (unpublished).
- 3. N. A. Uckan, ELMO Bumpy Square, ORNL/TM-9110, Oak Ridge National Laboratory (1984).
- 4. S. J. SACKETT, EFFI-A Code for Calculating the Eletromagnetic Field, Force, and Inductance in Coil Systems of Arbitrary Geometry, Lawrence Livermore Laboratory Report, UCRL-52404, Rev. 1 (1981).

ORNL/TM-9542 Distribution Category UC-20d

INTERNAL DISTRIBUTION

- 1-3. L. S. Abbott
 - 4. F. S. Alsmiller
 - 5. R. G. Alsmiller, Jr.
 - 6. J. M. Barnes
 - 7. L. A. Berry
 - 8. W. E. Bryan
 - 9. R. A. Dory
- 10. J. D. Drischler
- 11-15. EPD Reports Office
 - 16. T. A. Gabriel
 - 17. W. Houlberg
 - 18. R. A. Lillie
 - 19. F. C. Maienschein
 - 20. L. W. Owen
 - 21. M. W. Rosenthal
 - 22. RSIC
- 23-27. R. T. Santoro
 - 28. J. Sheffield

- 29. D. A. Spong
- 30-34. N. A. Uckan
 - 35. T. Uckan
 - 36. A. Zucker
 - 37. P. W. Dickson, Jr. (Consultant)
 - 38. G. H. Golub (Consultant)
 - 39. D. Steiner (Consultant)
- 40-41. Central Research Library
 - 42. Fusion Energy Division Library
 - 43. Fusion Energy Division Reports Office
 - 44. ORNL Y-12 Technical Library
 Document Reference Section
- 45-46. Laboratory Records
 - 47. ORNL Patent Office
 - 48. Laboratory Records RC

EXTERNAL DISTRIBUTION

- 49. Office of Assistant Manager for Energy Research & Development, DOE-ORO, Oak Ridge, TN 37830.
- W. B. Ard, McDonnell Douglas Astronautics Co., PO Box 516, St. Louis, MO 63166
- 51. S. E. Berk, Division of Development and Technology, Office of Fusion Energy, ER-532, U.S. Dept. of Energy, Washington, D.C. 20545.
- 52. J. D. Callen, Dept. of Nuclear Engineering, University of Wisconsin Madison, WI 53706.
- 53. R. W. Conn, Dept. of Chemical, Nuclear, and Thermal Engineering, University of California, Los Angeles, CA 90024

- 54. R. A. Dandl, Applied Microwave Plasma Concepts, Inc., 2210 Encinitas Blvd. Encinitas, CA 92024
- S. O. Dean, Director, Fusion Energy Development, Science Applications, inc., 2 Professional Dr., Suite 249, Gaithersburg, MD 20760.
- 56. D. G. McAlees, Exxon Nuclear Co., Inc., 777 106th Ave., N Bellevue, WA 98009.
- 57. Library, Princeton Plasma Physics Laboratory, Princeton University, P.O. Box 451, Princeton, NJ 08540.
- 58-59. R. J. Schmitt, McDonnell Douglas Astronautics Co., PO Box 516, St. Louis, MO 63166
 - 60. Dr. Yasushi Seki, Japan Atomic Energy Research Institute, Tokai-mura, Ibaraki-ken, Japan.
 - 61. W. M. Stacey, Jr., School of Nuclear Engineering, Georgia Institute of Technology, Atlanta, GA 30332.
 - 62. J. M. Turner, Office of Fusion Energy, Office of Energy Research, Mail Station G-256, U.S. Dept. of Energy, Washington, DC 20545
- 63-191. Given distribution as shown in TID-4500, Magnetic Fusion Energy (Distribution Category UC-20d: Fusion Systems).